EFFECTS OF NEAR-FIELD OBSTACLES ON FAR-FIELD ANTENNA PERFORMANCE CHARACTERISTICS*

F.L. Cain, B.J. Cown, and E.E. Weaver
Radar Division
Georgia Institute of Technology
Atlanta, Georgia 30332

E.F. Duffy
Naval Ship Engineering Center
Hyattsville, Maryland 20782

Summary

Considerable research has been conducted to investigate near-field coupling between antennas, both with and without obstacles located in the near-field of the antennas, but until now, very little research has been conducted to provide information for predicting the effects of various near-field obstacle blockages on far-field antenna performance characteristics. Recently completed research investigations at Georgia Tech for the U. S. Naval Ship Engineering Center have yielded considerable design information and have provided much insight into potential problem areas such as those dealing with near-field obstacles and their effects on far-field gain loss, beamwidths, beamshifts, and maximum sidelobe levels. The effects of several variables on these far-field antenna performance characteristics were investigated, and various trends as well as typical design curves will be discussed. The usefulness of the information is illustrated by insertion of the far-field gain-loss data into a computer program for shipboard siting of antennas. Moreover, based on theoretical and experimental investigations with a dielectric-coated solid metal circular mast, applications of dielectric coatings to portions of ship superstructures to improve the far-field antenna performance is possible. A correlation of the effects of near-field obstacles on far-field antenna characteristics and on near-field antenna-to-antenna coupling is also possible.

Introduction

The topside placement of shipboard antennas to obtain acceptable electromagnetic performance still remains a critical problem. The magnitude of the topside electromagnetic problem arises because of various reasons. Among these are the large number of antennas that must be installed in a limited physical space, the unknown interactions among various antennas due to energy at both in-band and out-of-band frequencies, and the many different obstacles and objects of various geometrical shapes and sizes that exist aboard ships. Although coupling between antennas can sometimes be reduced by taking advantage of blockage due to parts of the ship, the far-field performance of an antenna can be degraded even though such undesired coupling is reduced. Thus, the EMC engineer and the radar systems engineer may be confronted with incompatible situations in the design and installation of new shipboard electronic systems.

Antenna performance data are necessary in order to determine what characteristics of an antenna are degraded due to obstacles in the vicinity of the antenna. The radar engineer must know the effects of these obstacles to determine if a particular radar can perform its functions satisfactorily and to what extent must corrective adjustments be made. Therefore, the effects of various obstacles on the antenna gain, beamwidth, beamshift, and close-in sidelobes must be known.

* This work was supported by the U.S. Naval Sea Systems Command, Washington, D.C.

Obstacle Investigations

Test Antennas, Obstacles, and Procedures

S-band (3000 MHz), C-band (5500 MHz), and X-band (9600 MHz) test antennas were used. The S-band and C-band antennas were both 4-foot paraboloidal dishes with F/D ratios of approximately 0.3 and are fed by slightly flared waveguide feeds. The X-band antenna is a parabolic-cylinder reflector fed by an X-band hoghorn feed; its maximum horizontal dimension is about 4.9 feet. The first two antennas above can accomodate either vertical or horizontal polarization. Seventeen obstacles (solid cylindrical masts, square columns, corner reflectors, wedges, open masts, and flat metal sheets) were utilized in the experiments. The widths of each type of obstacle were 6 inches, 24 inches, and 48 inches, except those for the open masts whose widths were 24 and 48 inches.

The measurement procedures were similar to those employed for previous near-field coupling tests [1-3], except that the transmitting antenna (for the results described in this paper) were always located in the far-field of the receiving antenna in order to simulate a return signal from a distant target. In the far-field measurements, each near-field obstacle was located approximately the same distance from the receiving antenna as it was was in the corresponding near-field antenna-coupling case. Each obstacles at each fixed near-field distance from the receiving antenna was moved in angular increments along an arc whose radius was measured from the center of the axis-of-rotation of the antenna positioner. The schematic diagram in Figure 1 illustrates the arrangement for the measurement procedure. At each near-field

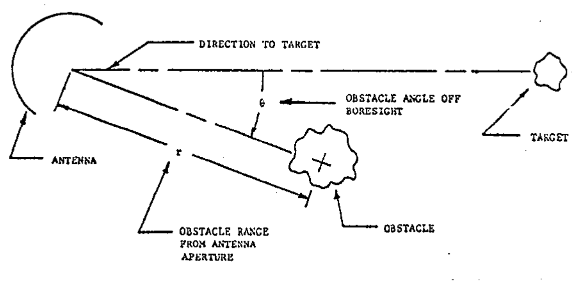

Figure 1. Simplified schematic illustrating far-field performance test variables for a simulated target return.

obstacle location, which includes locations along the direction toward the transmitting antenna (target), far-field antenna patterns were recorded about the boresight direction to the target.

Antenna Performance Displays for Solid Obstacles

The ability to predict the effects of obstacles in the near-field of an antenna on the far-field performance of the antenna is an important capability for improving the electromagnetic effectiveness of future topside designs. The position of the null of a monopulse or a conically scanned antenna, for example, is very important in a tracking mode. Consequently, if an obstacle were located on one side of the line-of-sight between the target and the antenna, the obstacle would affect the return signal from the target more on one side of the antenna pattern than on the other side. Therefore, the pattern null would shift, and a tracking-angle error would result.

To determine the magnitude of the detrimental effects that can be caused by nearby obstacles, a series of far-field antenna performance experiments involving various obstacles at several near-field ranges were conducted for in-band frequencies [1,4]. The same near-field objects that were used in the corresponding antenna-to-antenna near-field coupling tests were used in the far-field performance tests. The effects of the various near-field obstacles on the far-field antenna performance are characterized in terms of decoupling (antenna gain loss), beamwidth, beamshift, and close-in sidelobe levels. In many situations, particularly when the width of the near-field obstacle is comparable in size to the antenna aperture, the distortion effects on the clear-site antenna pattern are very complex. The inherent complexity which often occurs demands the use of engineering judgments in interpreting and using these far-field antenna performance descriptors. Use of the various empirical curves should be guided by the radar system accuracy requirements. A good engineering description demands that all appropriate empirical performance data be consulted.

Main-Beam Boresight-Decoupling Displays The main-beam boresight-decoupling data are displayed in two different formats. In the first format, displays such as shown in Figure 2 permit easy visualization of the manner in which the decoupling values change with increasing obstacle distance from the receiving antenna and easy comparison with near-field antenna-to-antenna boresight decoupling.

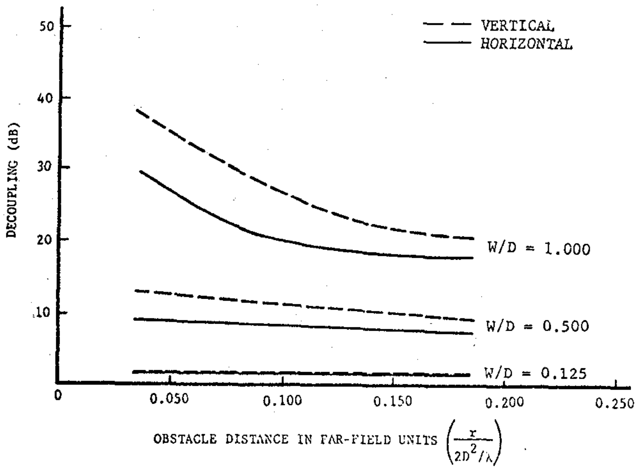

Figure 2. Average boresight decoupling as a function of obstacle distance along boresight direction (target direction) for receiving antenna aperture D for the Mast obstacles of widths W for vertically and horizontally polarized signals at a frequency of 3000 MHz. Receiving antenna is in far field of target.

In the second format, displays as shown in Figure 3, with near-field obstacle distance as the parameter, were derived to portray the decoupling values as a function of the angle from which the near-field obstacle is removed from the boresight direction.

Decoupling along Boresight In all cases, the boresight decoupling for all three sizes of obstacles for both horizontal and vertical polarization is displayed as a function of the obstacle distance, r, from the receiving antenna normalized in far-field units of $2D^2/\lambda$, where D is the horizontal dimension of the receiving antenna and λ is the operating wavelength. The curve

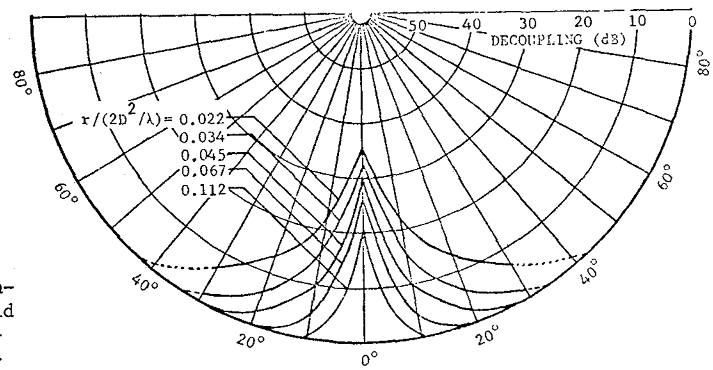

Figure 3. Average boresight decoupling as a function of the angle between obstacle and target direction for mast and sheet obstacles of normalized width 1.0 for indicated normalized obstacle distances from receiving antenna aperture D and for horizontally polarized signals at a frequency of 5500 MHz.

parameter for the obstacles is the width of the particular obstacles, W, normalized in terms of the horizontal dimension of the receiving antenna.

The trend of the data displayed in Figure 2 is in general typical. Greater decoupling occurs for vertically polarized signals than for horizontally polarized signals, but the difference generally decreases as the size of an obstacle decreases. In all cases, the decoupling levels are larger for larger size obstacles than for smaller size obstacles. The slopes of the decoupling curves generally tend to be negative (that is, the decoupling values decrease as the distance of the obstacle from the receiving antenna increases) and tend toward larger values as the size of an obstacle increases. For a given frequency of operation, major differences between decoupling levels are likely to occur for same-size obstacles of different types if one of the obstacles is a square column whose W/D ratio is one and if the polarization is vertical. The differences become less distinct for horizontal polarization and for smaller W/D ratios for either polarization.

The S-band boresight decoupling data indicate one trend not observed in the C-band and X-band data. For larger obstacles, W/D = 1, the slopes of the S-band curves for both vertically-polarized and horizontally-polarized signals generally are not linear. This trend implies that the decoupling level as a function of the obstacle distance from the receiving antenna along the boresight direction monotonically decreases and approaches a limiting value. In terms of the far-field units of $2D^2/\lambda$, the maximum obstacle distance from the receiving antenna is considerably greater at the S-band frequency than at either the C-band or X-band frequency. Based on the S-band data, it appears that approximately 0.2 of the far-field distance may be a good rule-of-thumb for the obstacle distance (break-distance) for which the boresight decoupling values approach a constant value. If this rule-of-thumb were true for all microwave frequencies, then a useful technique for application in topside design would exist. However, further investigations should be conducted to substantiate this conjecture.

Decoupling Versus Obstacle Angle Observations of the experimental data indicate that several trends are self-evident, while others are more subtle. As the obstacle angle off the boresight direction to the target increases, the decoupling (peak gain loss) decreases for all obstacle sizes, obstacle distances, polarizations, and frequencies. It is also evident that a given level of decoupling is dependent on the obstacle width and the obstacle distance from the antenna. A W/D ratio of unity yields a larger decoupling value than a W/D ratio of 0.5 or of 0.1, as one would expect.

Although the electrical distance of a given obstacle from an antenna [in terms of $r/(2D^2/\lambda)$] appears to be a major factor in determining the maximum decoupling at 0°, the physical distance appears to be a major factor in determining the extent of the angular blockage. It appears that as the obstacle distance from the receiving antenna approaches relatively large values, the maximum decoupling approaches a limiting value and the extent of the angular blockage decreases to zero, that is, there would be no blockage except at 0° on the polar plot; however, the magnitude of decoupling value may depend on the size of obstacle, the type of obstacle, the frequency, and the polarization. Additionally, in this limiting case, the obstacle itself must remain in the far-field of the target as the obstacle distance from the receiving antenna increases.

Maximum Sidelobe-Level Displays The manner in which the maximum radiation-lobe on both sides of the boresight direction (direction to the target) as a function of the obstacle angle off the boresight direction can vary is displayed in Figure 4. In this display, the

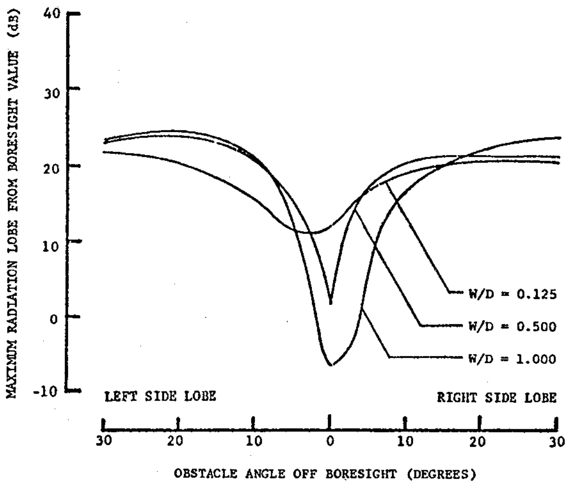

Figure 4. Maximum radiation-lobe levels to the left and right of boresight as a function of obstacle angle off boresight for horizontally polarized signals for the indicated normalized obstacle widths at the normalized near-field range of 0.034 at 5500 MHz. The positive values of the ordinate indicate the level down from boresight value.

obstacle angle off boresight is positive both to the right and left of zero degrees. This interpretation must be used because the obstacle was always located on the right-hand side of direction to the target as viewed from the receiving antenna. Therefore, the interpretation of the left sidelobe on the display is the effect on the left sidelobe of a radiation pattern that an obstacle on the right-hand side of boresight produces. Similarly, the right sidelobe on the display must be interpreted as the effect on the right sidelobe of a radiation pattern that an obstacle located on the right-hand side of boresight produces. In the figure, the normalized width of the obstacle is the parameter. Because the raw data indicate that the maximum sidelobe levels do not strongly depend on the type of obstacle, each curve is an average curve derived by averaging the maximum sidelobe values of all types of obstacles of a given size.

The general trends of the curves (typically illustrated by Figure 4) in each frequency group are similar. As expected, the most severe degradations generally occur in the neighborhood of boresight. In the figure, the positive values for the maximum radiation lobe indicate the values down from the value on antenna physical boresight. Consequently, the negative values, which only occur for obstacles whose W/D ratio is approximately unity, indicate that maximum radiation lobe values are greater than those which occur at the physical boresight direction (i.e., this can be interpreted as a shifted main beam). The left and right sidelobes are affected differently for a given obstacle angle off boresight as the receiving antenna is rotated in the horizontal azimuthal plane. Also, an obstacle located near the antenna affects the maximum sidelobe level over a larger sector than does an obstacle farther away from the antenna.

Half-Power Beamwidths For a given obstacle distance, obstacle size, obstacle angle, and polarization, the beamwidths as a function of obstacle angle off boresight for all the obstacles were averaged to derive curves as illustrated in Figure 5. The square column obstacle

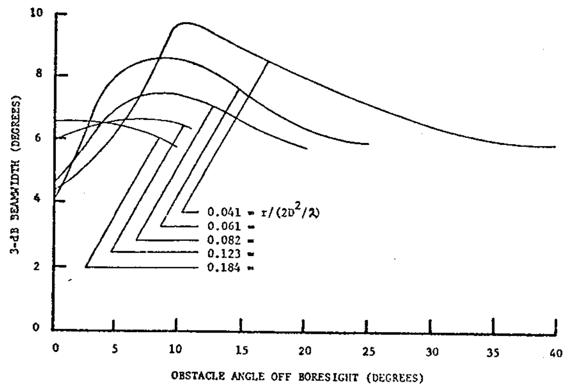

Figure 5. Half-power beamwidth as a function of obstacle angle off boresight for the indicated normalized obstacle distances. The levels for each obstacle of normalized width of 0.500 were combined for vertically polarized signals at 3000 MHz.

located in the near field of an antenna generally affected the far-field antenna pattern to a larger extent than did the other obstacles, particularly for short obstacle distances and small obstacle angles on or off the boresight direction. When the degradations approached a certain stage, no attempts to approximate the 3-dB beamwidths for this obstacle were made.

Several general trends were noted. For the largest-size obstacles (W/D≃1), the beamwidth is largest when the obstacle is located on boresight but decreases toward the clear-site beamwidth as the obstacle angle increases. However, for the middle-size obstacles (W/D≃0.5) as indicated in Figure 5, and smallest-size obstacles (W/D≃ 0.125), the beamwidths on boresight tend to be less than the clear-site beamwidths, reach maximum values at intermediate angles off boresight, and then approach the clear-site beamwidth values as the obstacle angles further increase. The clear-site 3-dB beamwidths of the antennas are approximately 5.5 degrees, 3.0 degrees, and 2.0 degrees for 3000 MHz, 5500 MHz, and 9600 MHz, respectively. The results from the overall research program also indicate that for a given obstacle angle, the differences between beamwidths as a function of near-field distance are generally greater for larger obstacles than for smaller-size obstacles. As a consequence, not much variance among the curves for the smallest obstacles at any of the three test frequencies occurs.

Beamshifts Experimental tests indicated that certain obstacles located in the near field of an antenna cause an angular shift (or scan) in the pointing direction of the main beam of the antenna. As a result, the return signal from a far-field target appears to be from a direction other than the true target direction; consequently, an error in bearing occurs. Tests indicate that the magnitude of the beamshift strongly depends on the normalized width (ratio of obstacle width to antenna aperture width) of the obstacle and on the obstacle angle off the boresight direction. For small normalized obstacle widths (W/D≃0.1), no significant beamshifts occur. For W/D ratios of approximately 0.5, small beamshifts much less than 0.5 degree apparently occured for obstacle angles near boresight, but no well-defined trends could be definitely established within the measurement accuracy achievable in these particular tests. However, for large obstacles whose W/D ratios are approximately unity, significant beamshifts occur. Consequently, the tests indicate that obstacles whose normalized widths are greater than 0.5 produce significant beamshifts and should be considered in electromagnetic effectiveness performance analyses.

Empirically-derived curves of beamshifts as a function of obstacle angle off the boresight direction (direction to the target) are displayed in Figure 6 for obstacles whose W/D ratios are unity. The near-field distance of the obstacles from the receiving antenna is the parameter in the family of curves, the polarization is horizontal, and the data for all types of obstacles for normalized width of unity were averaged for each polarization. The dashed lines of Figure 6 indicate that the square column obstacle data were not used; however, the solid portion indicates that all data were used in the empirical derivation of the average curves.

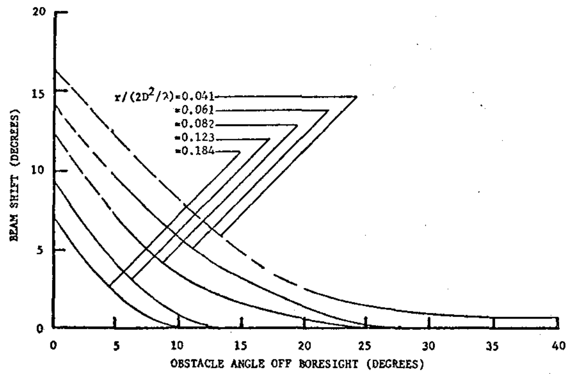

Figure 6. Beamshift as a function of obstacle angle off boresight for the indicated normalized obstacle distances. The levels for each obstacle of normalized width of 1.000 were combined for horizontally polarized signals at 3000 MHz.

Open-Mast Obstacle Tests

Open-mast investigations were conducted to acquire information similar to that acquired for the totally enclosed, solid-metal, near-field obstacles. The open-mast type of intervening near-field obstacles is an important obstacle in which very little experimental or theoretical information exists. Estimates of open-mast blocking effects on the main-beam gain previously have been based on aperture blocking theory that is normally used only in the design of directive antennas for clear-site operation. Two types of open-mast structures were selected, designed, fabricated, and tested at the frequencies of 3000 MHz, 5500 MHz, and 9600 MHz. The geometry selected for the open mast was similar to that selected for the Patrol Frigate (PF)[5].

Two open masts were constructed to project blockages of about 22 percent and 28 percent onto the aperture of a 4-foot paraboloidal dish antenna. Because the horizontal widths of these open-mast structures coincide with the widths of the 24-inch and 48-inch wide solid obstacles, a data comparison is possible. Furthermore, the selection of these open-mast structures permit the effects of different distributions of aperture blockages to be observed. In addition, the effects of the total percentage of aperture blockage can be observed not only between the two open masts but also between a given open mast and a solid obstacle.

Although neither changes in beamwidths nor changes in beamshifts occurred, the overall trend of the gain-loss data along the boresight direction for the open masts is considerably different than that for the solid obstacles. For the open masts, there are usually only minor differences between W/D ratios of 0.5 and 1.0, and only very minor differences occur among the data for horizontally and vertically polarized signals. Further, the decoupling levels (gain loss) for the 24-inch and 48-inch open masts, particularly for S-band and C-band signals, are approximately the same as those for 6-inch solid obstacles.

The decoupling curves for average boresight decoupling as a function of the obstacle angle for the two open masts for the various near-field distances, polarizations, and frequencies show that the decoupling levels for the various situations do not always decrease monotonically to zero as the obstacle angle increases. This behavior is in direct contrast to the curves for solid obstacles. The most consistent trend appears to be that peak decoupling values occur at progressively larger obstacle angles as the near-field obstacle distance decreases. In addition, the peak values of the irregular curves tend to occur at smaller obstacle angles for smaller W/D ratios.

The maximum sidelobe levels on both sides of the main beam as a function of the angle that the obstacle is displaced from the target direction (boresight direction) are typically illustrated in Figure 7. It is important to note in the display that the obstacle angle off boresight is positive both to the left and to the right of zero degrees and should be interpreted in the same manner as previously described. In general, the manner in which an individual curve varies depends on the clear-site antenna pattern, the width of the open mast, and the near-field distance from the receiving antenna. The effects due to the open masts are generally the greatest for antennas with very low clear-site sidelobe levels. For shorter near-field obstacle distances, the sidelobes are affected over larger obstacle angles, as one would expect. Also, shorter obstacle distances and greater obstacle widths generally produce greater effects on the sidelobes over larger obstacle angles. Because the left sidelobe of the receiving antenna pattern was directed toward the transmitting antenna (target) at the same time the main beam of the receiving antenna was directed toward an open-mast obstacle that was always on the right-hand side of a straight line between the physical locations of the transmitting and receiving antenna, the left-hand sidelobes are more adversely affected for greater obstacle angles than are the right-hand sidelobes.

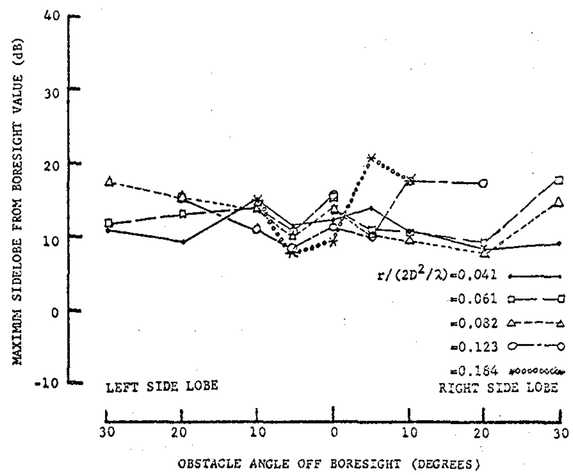

Figure 7. Maximum sidelobe level to the left and right of boresight as a function of obstacle angle off boresight; the positive values of the ordinate indicate the level down from the boresight value. Each curve in the family is for the open mast obstacle of normalized width 1.000 at the indicated normalized obstacle distances for 3000 MHz.

The data for both the 24-inch wide and 48-inch wide open masts indicate that sidelobes are usually down at least 10 dB from the peak of the main beam. This behavior is in direct contrast to that for solid obstacles of corresponding widths for which a wide variation in sidelobe levels occurs, particularly for small obstacle angles. The sidelobe levels for these two different open masts compare more closely to 6-inch wide solid obstacles than to either 24-inch or 48-inch wide solid obstacles. For a given frequency and open-mast width, no well-defined distinction between the cases for horizontal and vertical polarizations can readily be made.

Computer Techniques for Predicting Gain Loss

A computer program for shipboard siting of antennas [2,6,7] is continually being adapted to make it more useful to describe the gain loss caused by obstacles which block directive antennas. The determination of gain loss versus antenna pointing angle is accomplished with this program by using a measured data base in S, C, and X radar bands for solid obstacles as well as the two open-mast structures. An overall flow diagram of the computer program is shown in Figure 8. Some of the data already have been useful in the estimation of the effective radar coverage of both search and tracking antennas on the Patrol Frigate.

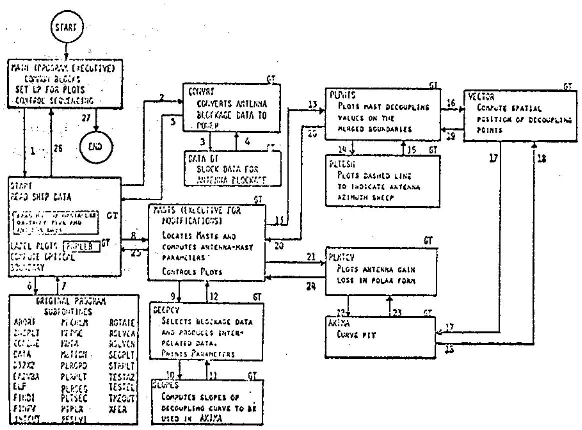

Figure 8. Over-all flow diagram of the computer-aided-ship-design (CASD) computer program after second modification.

Dielectric-Coat Obstacle Investigations

Theoretical and experimental studies conducted by Georgia Tech indicate that applying dielectric coatings to metal obstacles is one possible technique for improving ship topside electromagnetic effectiveness of directive antennas. A limited theoretical investigation for one specific dielectric-coated metal mast indicated that in general, significant improvements are possible. In particular, a one-way improvement of 20 dB in the field strength at the near-field point of interest behind the obstacle for vertical polarization and an isolation of 15 dB at the same near-field point for horizontal polarization were predicted. Analysis of the equations, as well as limited data, further indicated that the judicious selection of other parameters could conceivably result in even greater field-strength enhancement and/or isolation.

An exhaustive discussion relating to the extensive theoretical and experimental investigations that are needed to completely define and characterize the potential beneficial scattering properties of dielectric-coated masts is beyond the scope of this paper. However, the results of the experimental investigations of a dielectric-coated mast obstacle specifically demonstrated the following.

(1) Thin dielectric coatings on a circular metal mast located in the near-field of a receiving antenna can enhance the propagation of vertically-polarized electromagnetic energy around the mast and reradiate it in the forward direction to produce a significant increase in received power.

(2) Thin dielectric coatings on a circular metal mast in the near field of an antenna can significantly diminish the amount of horizontally polarized electromagnetic energy which would normally propagate around the mast and then be radiated from it in the forward direction, thus resulting in a significant increase in isolation.

(3) The beneficial effects of EM field enhancement and isolation produced by the dielectric coating can extend over a wide frequency range and over a wide range of near-field obstacle locations on boresight.

(4) The beneficial effects tend to be greater for obstacle locations which are physically closer to the receiving antenna where bare metal obstacles generally cause the greatest degradation of antenna performance.

These investigations were restricted to antennas and circular masts of small electrical dimensions for which relatively small improvements in boresight performance are predicted, as illustrated in Figures 9 and 10 for vertically and horizontally polarized incident signals, respectively.

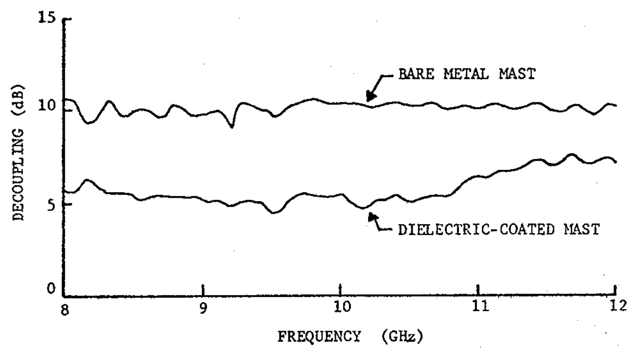

Figure 9. Boresight decoupling versus frequency for both a bare metal mast and dielectric-coated mast for vertically polarized incident signals.

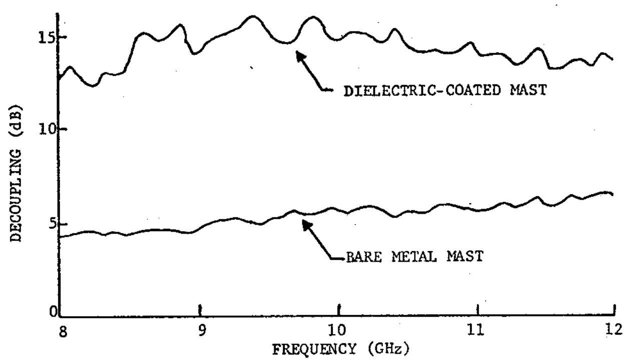

Figure 10. Boresight decoupling versus frequency for both a bare metal mast and dielectric-coated mast for horizontally polarized incident signals.

A Correlation Method

A typical procedure for correlating the results of the near-field coupling tests and the far-field performance tests is illustrated. The results of the near-field decoupling tests reveal that the various obstacles could be used to reduce electromagnetic interference between two antennas, whereas the results of the antenna performance tests demonstrate that these same obstacles could have degrading effects on antenna performance. Moreover, the possibility of degradations depends both on the angular coverage of the antenna and on the direction of the target relative to the obstacle, thus; there often is a need to correlate the results of both types of tests so that tradeoff criteria may be established. Decisions of an acceptable degree of compatibility and of an acceptable level of antenna performance will, of course, depend on the particular situation of interest and will have to be made by the engineers involved with the specific problem.

A hypothetical situation will be postulated to illustrate the type of logic used to correlate results and establish tradeoffs. Suppose it were desirable to locate a 48-inch mast directly between two 4-foot C-band dish antennas in order to obtain at least 35 dB of isolation between the antennas. One of these antennas must scan an azimuthal angular sector of ±30° relative to a specified direction; the mast is located at θ=20° from the center of the scan sector, as illustrated in Figure 11. Suppose a design requirement of the radar

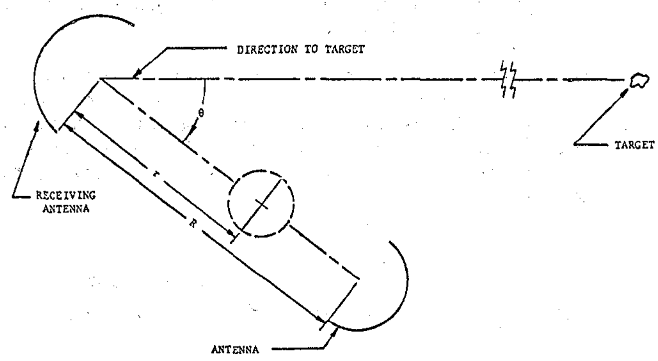

Figure 11. Schematic depicting a hypothetical situation to illustrate the correlation between the near-field and far-field empirical curves.

system engineer is that only a 3-dB degradation in gain due to the mast is tolerable when the scanning antenna is within ±10 degrees of the center of its scan sector. Outside the ±10 degree sector, stringent gain specifications are not necessary.

If the C-band frequency of operation of the radar antenna, designated as the receiving antenna in Figure 11, were 5500 MHz and the polarization of the antenna pair were horizontal, the EMC engineer would use the curve of Figure 12 to determine the obstacle separation distance necessary to produce a 35-dB main-beam decoupling. In this figure, 35-dB decoupling distance of (0.067) $(2D^2/\lambda)$, which is about 12 feet. Therefore, the EMC engineer must locate the 48-inch diameter mast about 12 feet from the receiving antenna to fulfill his requirement.

For this mast, frequency, and polarization, the radar systems engineer must use the polar-form decoupling curves of Figure 3 to determine the extent of degradation to the peak antenna gain of the scanning antenna. The greatest degradation to the peak antenna gain, within ±10 degrees of the center of the scan sector, will occur when the antenna has scanned 10 degrees toward the mast. Since the mast is located 20 degrees from the center of the scan sector, the mast is still 10 degrees from the antenna's boresight direction. Consequently, the curve corresponding to a normalized obstacle distance of 12 feet indicates a decoupling of about 4 dB for an obstacle angle of 10 degrees. This magnitude of decoupling marginally exceeds the 3-dB requirement. A possible trade-

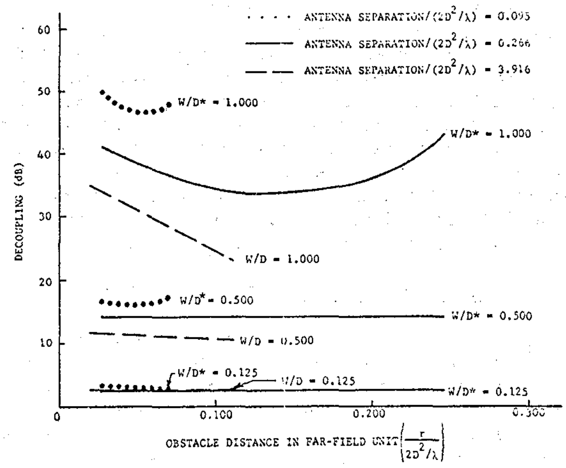

Figure 12. Average boresight decoupling as a function of obstacle distance along boresight from the receiving antenna aperture D for various mast widths W, for the three indicated antenna separation distances, and for horizontally polarized signals at a frequency of 5500 MHz. The transmitting and receiving apertures D were both 4.0 feet.

off might be to move the mast and transmitting antenna an additional 15 degrees from the center of the scan sector. As Figure 3 indicates at 15 degrees, about 2 dB of decoupling would occur for this situation; however, the mast still provides at least 35-dB isolation when the two potentially interfering antennas are on a common boresight.

For other specified requirements such as those for beamwidths, beamshifts, and maximum sidelobe levels, the combined use of the near-field and far-field curves can also be used in a similar manner. Therefore, the determination of a compatible arrangement, which may involve various tradeoffs, can be decided.

Concluding Remarks

Experimental investigations have yielded much design information concerning the effects of near-field obstacles on the far-field performance of antennas. Effects on performance are related (1) to the near-field obstacle size relative to the antenna aperture size, (2) to the near-field obstacle distance and angle off the boresight of the antenna, (3) to the polarization sense, (4) to the frequency of operation, and (5) to the geometry of the near-field obstacle. The far-field performance data in conjunction with previously derived near-field antenna-to-antenna coupling data are useful in the siting of shipboard antennas. Moreover, additional investigations concerning dielectric-coated obstacles to improve antenna performance have yielded encouraging results. Data of these types are adaptable for insertion into a computer program for shipboard siting of antennas.

References

1. F.L. Cain, C.E. Ryan, C.P. Burns, and B.J. Cown, "Near-Field Obstacle Effects and Phased-Array Studies," Final Engineering Report, Contract No. N00024-71-C-1120, Georgia Institute of Technology, January 1972.

2. F.L. Cain, C.E. Ryan, B.J. Cown, and E.E. Weaver, "Electromagnetic Effectivness Investigations of Near-Field Obstacle Effects, Antenna Coupling, and Phased Arrays," Final Engineering Report, Contract No. N00024-72-C-1274, Georgia Institute of Technology, June 1973.

3. F.L. Cain, B.J. Cown, and E.E. Weaver, "Out-of-Band-Frequency Investigations of Near-Field Obstacle Effects and Phased Arrays," Final Engineering Report, Contract No. N00024-73-C-1141, Georgia Institute of Technology, February 1974.

4. F.L. Cain, B.J. Cown, E.E. Weaver, and C.E. Ryan, "Far-Field Antenna Performance Investigations Concerning In-Band Effects of Near-Field Structures and Out-of-Band Phased Arrays," Final Engineering Report, Contract No. N00024-74-C-1215, Georgia Institute of Technology, January 1975.

5. C.E. Ryan and R.D. Nevels, "Final Report Consulting Services in Support of the Patrol Frigate Electromagnetic Effectiveness Analysis Program," Georgia Institute of Technology, Final Report, Subcontract No. A2MV-568343 to Prime Contract No. N00024-72-C-1444, August 1973.

6. T.F. Schmeckpeper and C.A. Bass, "A Computer Method for Shipboard Siting of Antennas," NRL Report 7144, 30 July 1970, Naval Research Laboratory, Department of the Navy, Washington D.C.

7. R.O. Niemi, "A Ship Modelling Program Description for the IBM/360/65," NELC Technical Note J411, 18 November 1971, Microwave Technology Division, (Code 2300), Naval Electronics Laboratory Center, San Diego, California 92152.